Supplementary Materials for

Inferring change points in the spread of COVID-19 reveals the effectiveness of interventions

Jonas Dehning*, Johannes Zierenberg*, F. Paul Spitzner*, Michael Wibral, Joao Pinheiro Neto, Michael Wilczek*, Viola Priesemann*†

*These authors contributed equally to this work.
†Corresponding author. E-mail: viola.priesemann@ds.mpg.de

Published 15 May 2020 on *Science* First Release
DOI: 10.1126/science.abb9789

This PDF file includes:

Other Supplementary Material for this manuscript includes the following:
(available at science.sciencemag.org/cgi/content/full/science.abb9789/DC1)

Table S1.

Table S1: Overview of model parameters.

Variable	Parameter
λ	Spreading rate
μ	Recovery rate
$\lambda^* = \lambda - \mu$	Effective spreading rate
λ_i	Spreading rate after i-th intervention
t_i	Time of i-th intervention
f_w	Amplitude of weekend corrections
Φ_w	Phase shift of weekend correction
σ	Scale factor of the width of Student's t-distribution
N	Population size (83.000.000)
S_t	Susceptible at time t
I_t	Infected at time t
R_t	Recovered at time t
Δt	Time step
$R_t^{\text{new}} = \mu \Delta t I_{t-1}$	New recoveries at time t
$I_t^{\text{new}} = \lambda \Delta t \frac{S_{t-1}}{N} I_{t-1}$	New infections at time t
$C_t = I_{t-D}^{\text{new}}$	New reported cases at time t
D	Delay of case detection

Table S2.

Table S2: Model comparison: Using leave-one-out (LOO) cross-validation, we compare our original "SIR main" model that features a weekend modulation (to account for fewer reported cases during weekends) with other model variants. Remarkably, the median inferred effective growth rate λ^* after the last change-point is very similar for all model variants. For full details on the model variants, see the figure captions in the SI: (i) SEIR-like with explicit incubation time, Fig. S3. (ii) SIR excluding the weekend modulation, Fig. S4. (iii) Sensitivity analysis by applying wider priors to different parameters, Figs. S5, S6, S7. Lower LOO-scores represent a better match between model and data (pLOO is the effective number of parameters).
[†]For the SEIR-like model, the magnitude of the effective growth rate is not directly comparable because of the explicit incubation period.

Model	# c-pts.	λ_0^*	λ_1^*	λ_2^*	λ_3^*	LOO-score	pLOO
SIR main	0	0.03				927 ± 9	8.31
SIR main	1	0.21	-0.03			819 ± 16	13.46
SIR main	2	0.30	0.11	-0.03		796 ± 17	12.53
SIR main	3	0.30	0.12	0.02	-0.03	787 ± 17	13.42
SIR without weekend modulation	3	0.31	0.13	0.04	-0.03	807 ± 17	9.65
SIR with wider delay prior	3	0.30	0.12	0.02	-0.04	787 ± 17	14.15
SIR with wider change point priors	3	0.30	0.12	0.02	-0.04	787 ± 17	14.29
SIR with wider transient length prior	3	0.29	0.12	0.02	-0.04	785 ± 17	13.92
SEIR-like[†]	3	1.95	0.45	0.05	-0.12	782 ± 17	10.71

Fig S1.

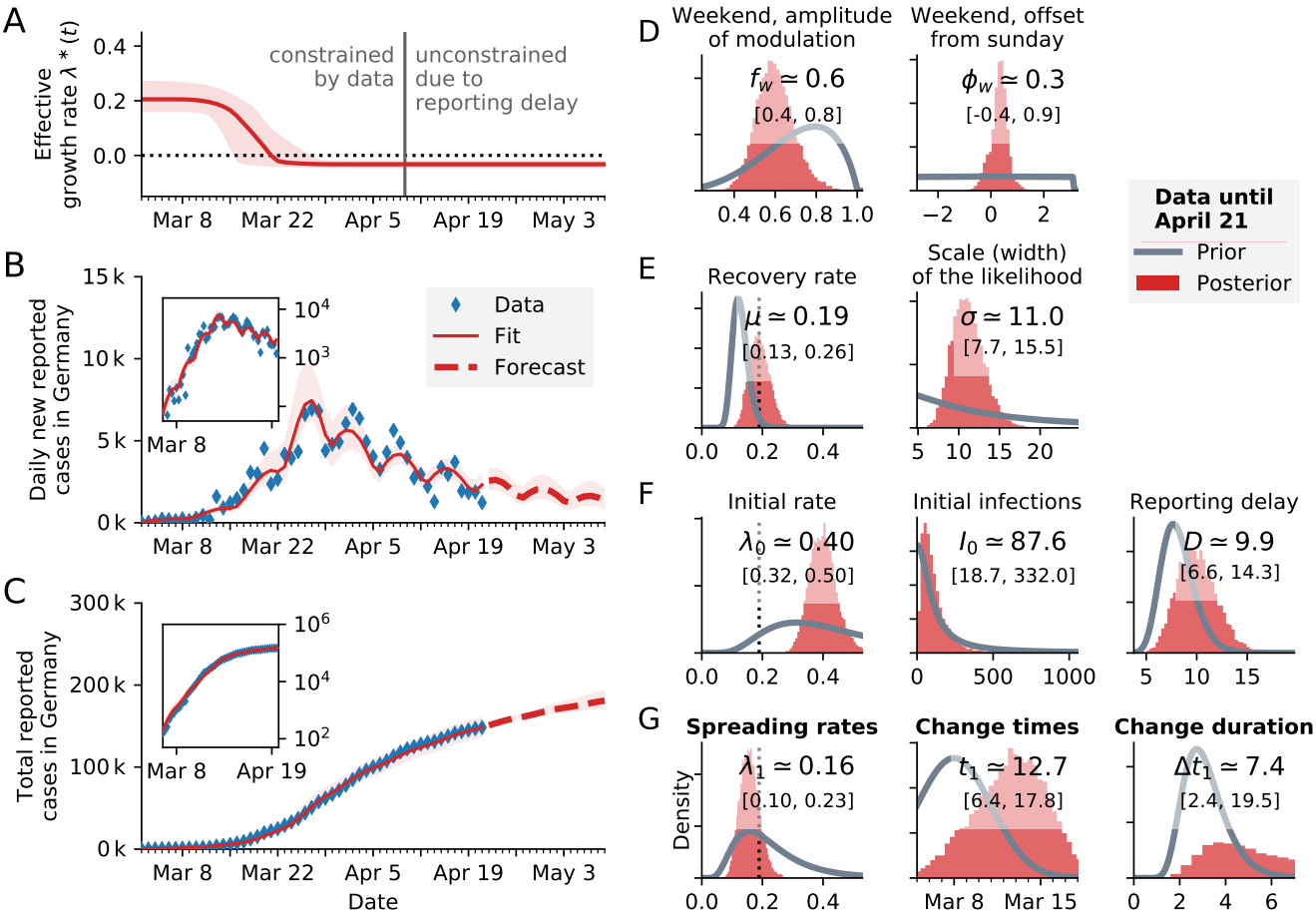

Figure S1: **Model comparison:** Change-point detection as in Fig. 3 (three change points, main text) with the **same model** "SIR main" but only **one change point**. With only one change point, the model cannot describe the data well after April 1. **A:** Time-dependent model estimate of the effective growth rate $\lambda^*(t)$. **B:** Forecast and comparison of daily new reported cases with the model fit, **inset:** Same on log-lin scale. **C:** Same as B but for cumulative (total) cases. **D–G:** Posterior distributions from the change point detection (red) compared to prior distributions (gray). Please refer to Fig. 1 (main text) for a more detailed description of the distributions.

Fig S2.

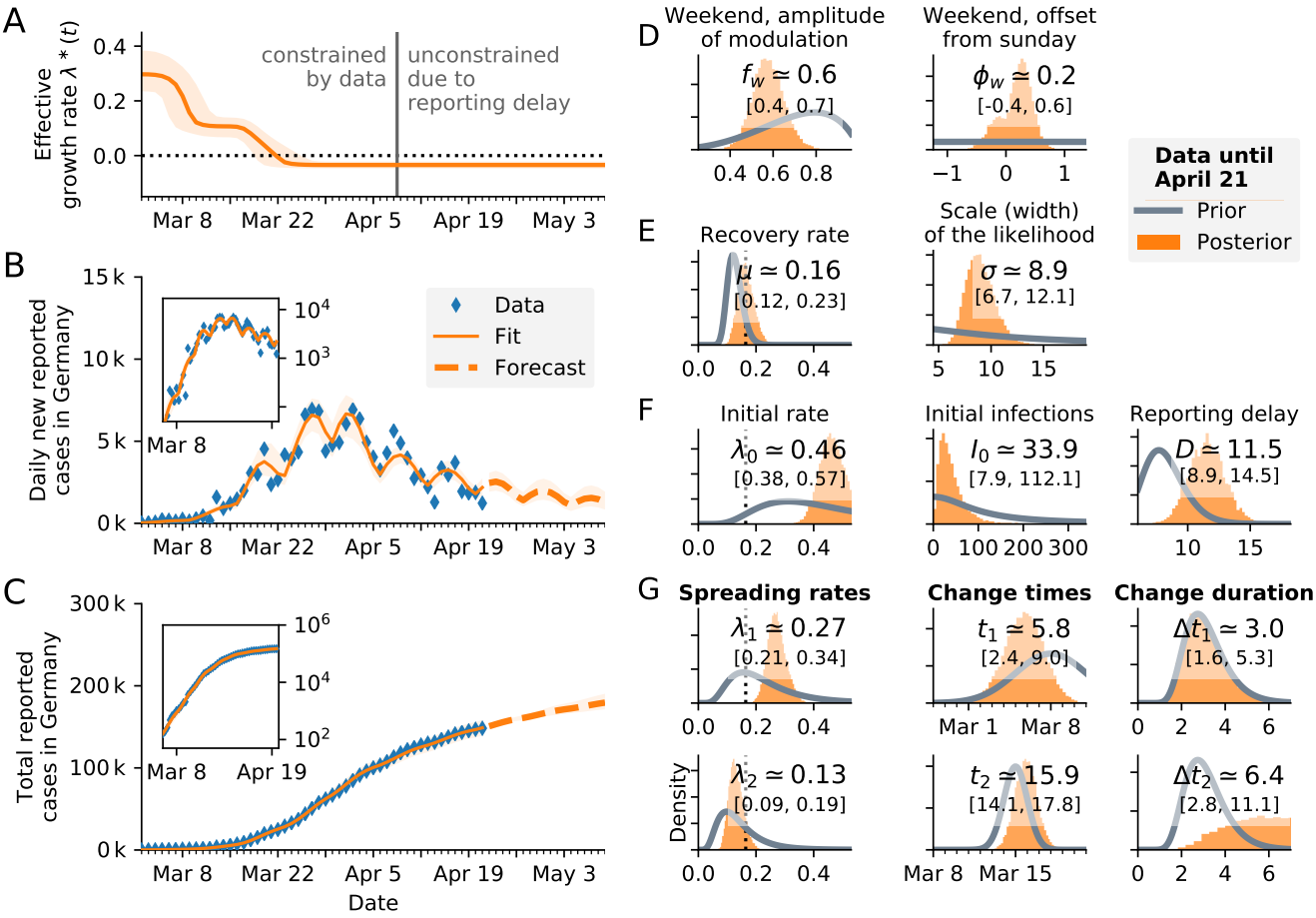

Figure S2: **Model comparison:** Change-point detection as in Fig. 3 (three change points, main text) with the **same model** "SIR main" but with **two change points**. With two change points, the onset time of the second change point is close to the (middle) one inferred when using the 3-c.p. model. However, the effective growth rate λ^* after the respective last c.p. is the same in both cases, $\lambda^* = -0.03$ (see also Table S2). **A:** Time-dependent model estimate of the effective growth rate $\lambda^*(t)$. Two change points are clearly visible. **B:** Forecast and comparison of daily new reported cases with the model fit, **inset:** Same on log-lin scale. **C:** Same as B but for cumulative (total) cases. **D–G:** Posterior distributions from the change point detection (orange) compared to prior distributions (gray). Please refer to Fig. 1 (main text) for a more detailed description of the distributions.

Fig S3.

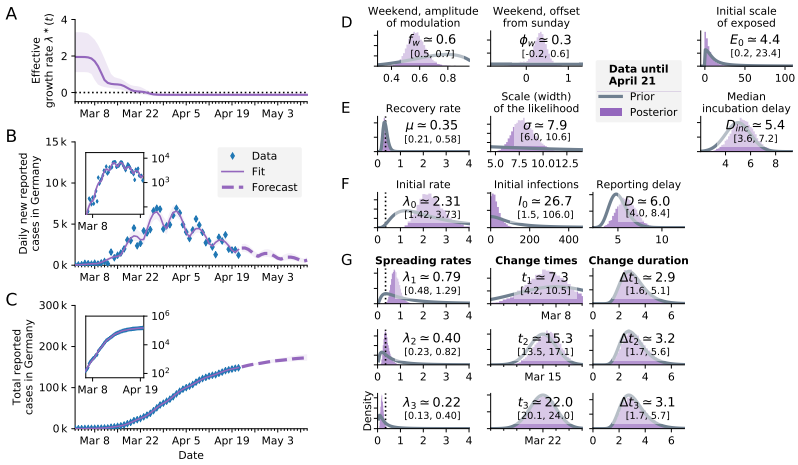

Figure S3: **Model comparison:** Change-point detection as in Fig. 3 (three change points, main text) but with a more involved **SEIR-*like*** model and **three change points**, code available online (*31*). Arguably, the SEIR-like model provides are more realistic (but also more complex) description of virus propagation. It yields a slightly better (lower) LOO-score than our "SIR main" model in the cross-validation, Table S2. However, inferred parameters are compatible with the simpler model and the inferred dynamics are similar. **Model details**: The SEIR-like model builds on our "SIR main" model (which includes a weekend correction, see Methods). The SEIR-like model features an explicit log-normal incubation period and a lognormal reporting delay. The incubation period is implemented as a discrete convolution of multiple exposed pools with a lognormal kernel. The discrete lognormal kernel is parameterized as follows (to match the characteristic incubation time of COVID-19 (*32*)): median D_{inc}, scale parameter 0.418 and normalized to 1. The median is a free parameter with prior Normal$(5,1)$ (days) (*32*). The reporting delay is implemented in a similar manner: as a convolution of the number of new cases with a lognormal kernel and the scale parameter is fixed to 0.3. In order to match the total delay of the main model (between the infection and the observation), the median D is a free parameter with prior LogNormal$(5,0.2)$ (days). Note that because of the lognormal-distributed incubation period in the SEIR-like model, the spreading and recovery rates are not directly comparable to the SIR models. We correspondingly adapted the respective priors (*17*): We adapted the prior median of the recovery rate μ to 1/3 with a scale factor of 0.3, and the prior median for λ_0, λ_1, λ_2, and λ_3 to 2.0, 1.0, 0.5 and 0.25, respectively, with a scale parameter of 1 each. **A:** Time-dependent model estimate of the effective growth rate $\lambda^*(t)$. **B:** Comparison of daily new reported cases and the model (inset: log-lin scale). **C:** As B but for total (cumulative) reported cases. **D–G**: Prior and posterior distributions of all free parameters.

Fig S4.

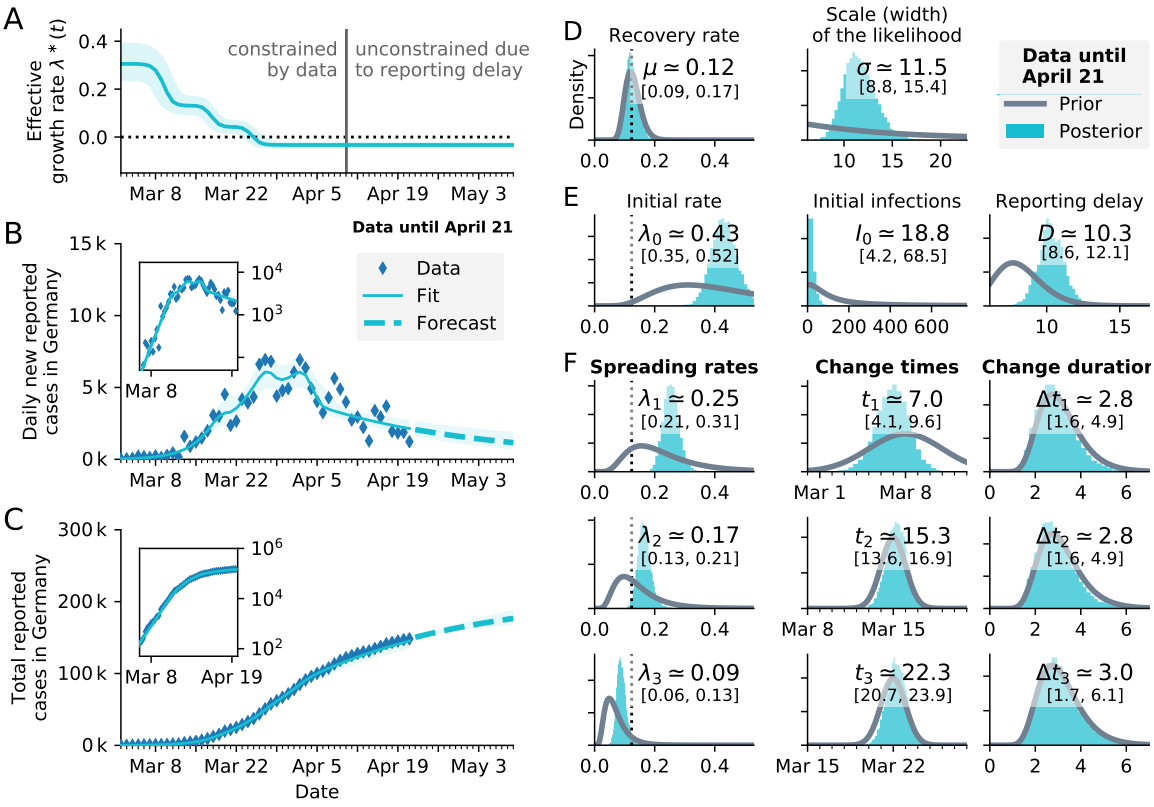

Figure S4: **Model comparison:** Change-point detection as in Fig. 3 (three change points, main text) with an **SIR model that excludes the weekend modulation** but features the **three change points**. In this version of the model, we excluded the assumption that daily new reported cases depend on the weekday (which is modeled as an absolute sine with an amplitude and a phase shift as inferred parameters in the main model). While the inferred parameters from the model that excludes the weekend modulation (in particular rates and onset times of change points) match the model that includes the modulation, the LOO-scores of the cross-validation are worse, Table S2. Especially in panel B it becomes clear that the (empirically motivated) dependence of reported on cases on the weekday is justified. Without the modulation, the model fit does not capture the periodic changes in the data. **A:** Time-dependent model estimate of the effective growth rate $\lambda^*(t)$. **B:** Comparison of daily new reported cases and the model (inset: log-lin scale). **C:** As B but for total (cumulative) reported cases. **D–F**: Prior and posterior distributions of all free parameters.

Fig S5.

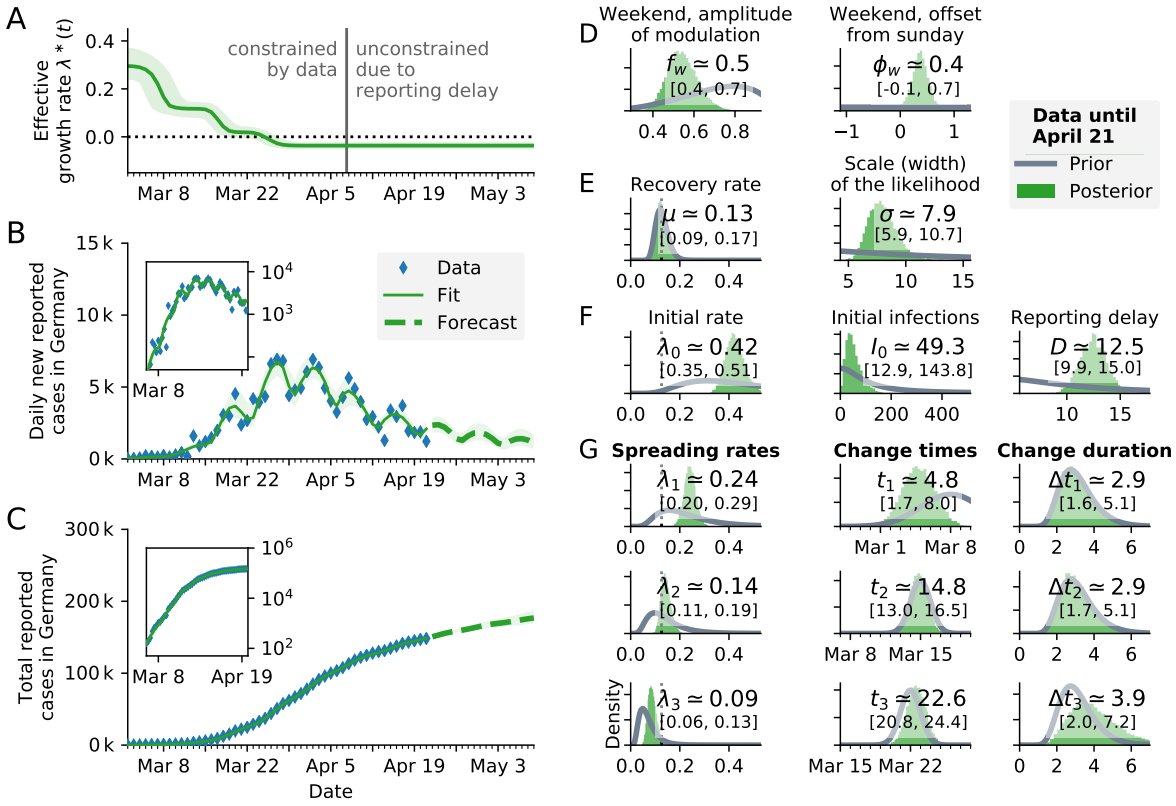

Figure S5: **Sensitivity analysis:** Change-point detection as in Fig. 3 (main text, three change points, same model) but with **a prior for the reporting delay that is 4 times wider** (panel F, third column). All parameters and change points are constrained by data. In particular, the posterior distribution of the reporting delay is slightly wider than with the original prior, but it is well constrained by data. **A:** Time-dependent model estimate of the effective growth rate $\lambda^*(t)$. **B:** Comparison of daily new reported cases and the model (inset: log-lin scale). **C:** As B but for total (cumulative) reported cases. **D–G**: Prior and posterior distributions of all free parameters.

Fig S6.

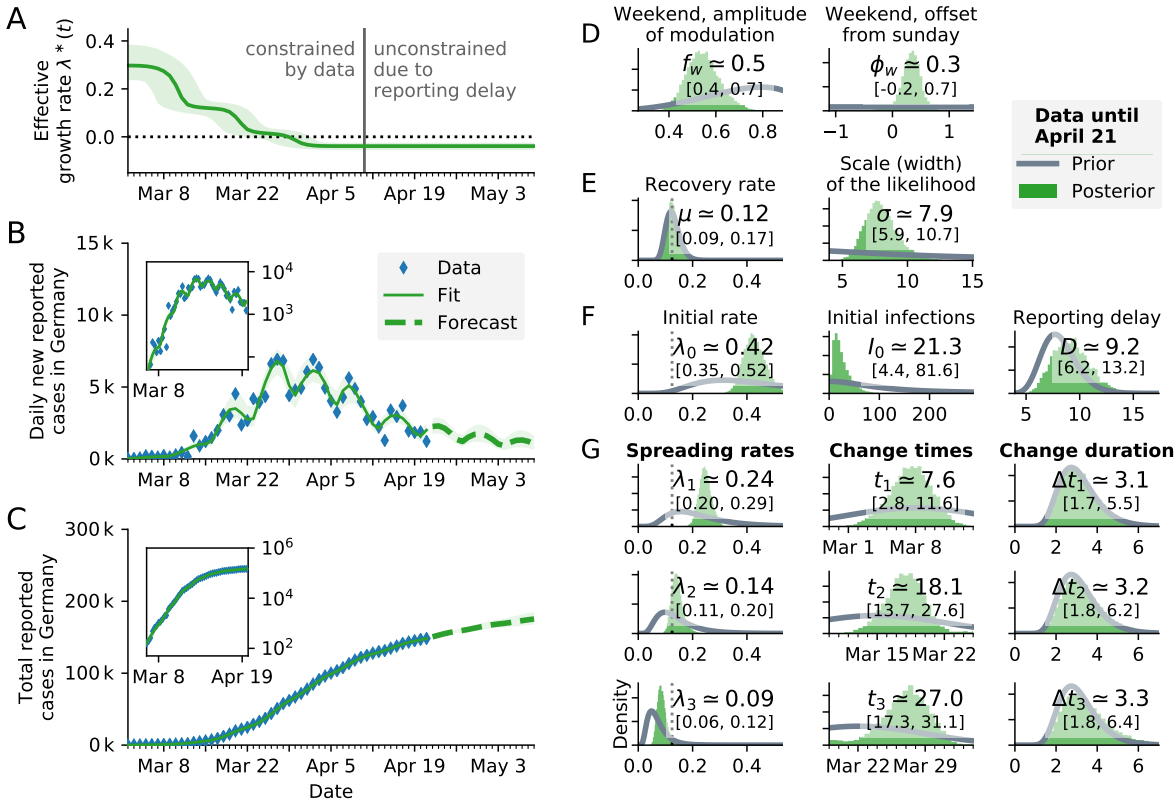

Figure S6: **Sensitivity analysis:** Change-point detection as in Fig. 3 (main text, three change points, same model) but with **a prior for the change times that is 14 days wide**, instead of ~ 2 days, (panel G, second column). All parameters and change points are constrained by data but the change points occur at later times compared to the original priors. **A:** Time-dependent model estimate of the effective growth rate $\lambda^*(t)$. **B:** Comparison of daily new reported cases and the model (inset: log-lin scale). **C:** As B but for total (cumulative) reported cases. **D–G**: Prior and posterior distributions of all free parameters.

Fig S7.

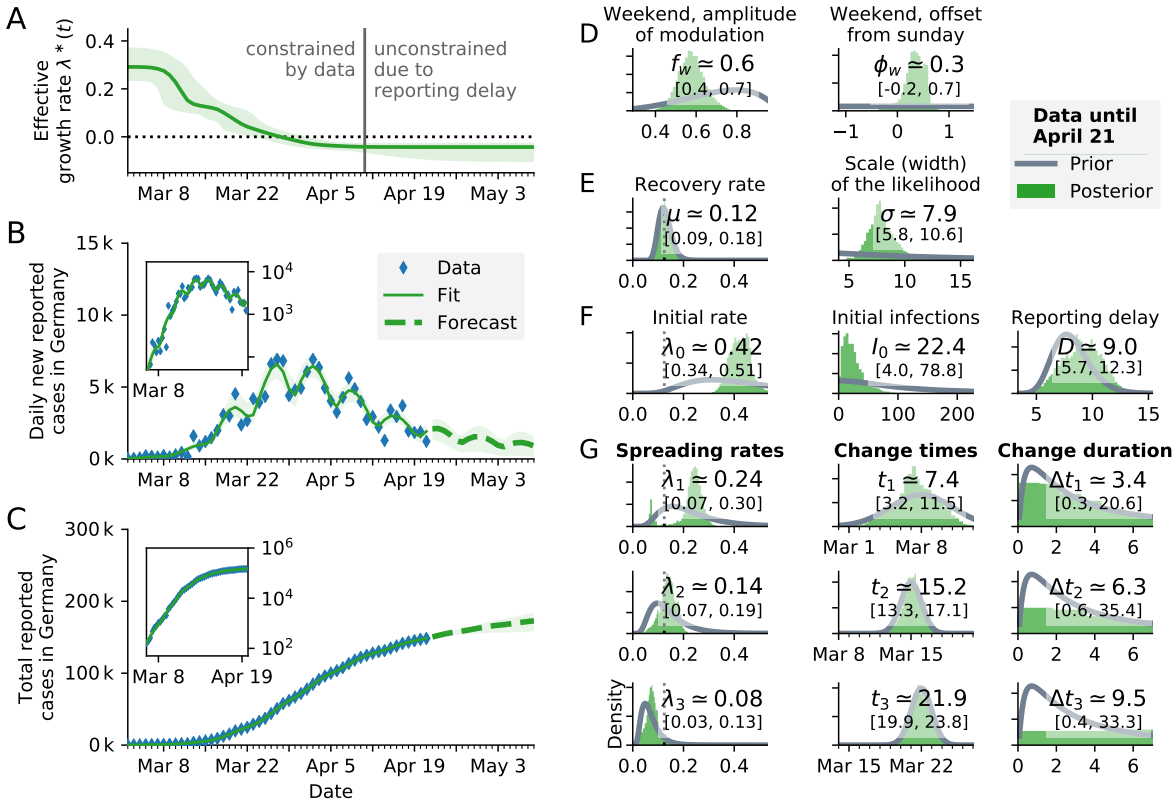

Figure S7: **Sensitivity analysis:** Change-point detection as in Fig. 3 (main text, three change points, same model) but with **a prior for the change duration that is 4 times wider** (panel G, third column). The duration of the first change point Δt_1 is robust to the wider prior; the data constrains the posterior. The durations of the second and third change point, Δt_2 and Δt_3 are not constrained by the data but they depend on our chosen priors. This is also visible in the lack of plateaus in the effective growth, panel A. However, the inferred spreading rate λ and the forecast are *not sensitive* to the wider priors. **A:** Time-dependent model estimate of the effective growth rate $\lambda^*(t)$. **B:** Comparison of daily new reported cases and the model (inset: log-lin scale). **C:** As B but for total (cumulative) reported cases. **D–G**: Prior and posterior distributions of all free parameters.

References and Notes

1. M. Enserink, K. Kupferschmidt, With COVID-19, modeling takes on life and death importance. *Science* **367**, 1414–1415 (2020). doi:10.1126/science.367.6485.1414-b Medline

2. E. T. Jaynes, *Probability Theory: The Logic of Science* (Cambridge Univ. Press, 2003).

3. A. Gelman, J. B. Carlin, H. S. Stern, D. B. Dunson, A. Vehtari, D. B. Rubin, *Bayesian Data Analysis* (CRC Press, ed. 3, 2013).

4. W. O. Kermack, A. G. McKendrick, G. T. Walker, A contribution to the mathematical theory of epidemics. *Proc. R. Soc. Lond. A* **115**, 700–721 (1927). doi:10.1098/rspa.1927.0118

5. H. Hethcote, The mathematics of infectious diseases. *SIAM Rev.* **42**, 599–653 (2000). doi:10.1137/S0036144500371907

6. J. Anderson, I. Lampl, I. Reichova, M. Carandini, D. Ferster, Stimulus dependence of two-state fluctuations of membrane potential in cat visual cortex. *Nat. Neurosci.* **3**, 617–621 (2000). doi:10.1038/75797 Medline

7. N. C. Grassly, C. Fraser, Mathematical models of infectious disease transmission. *Nat. Rev. Microbiol.* **6**, 477–487 (2008). doi:10.1038/nrmicro1845 Medline

8. R. Parshani, S. Carmi, S. Havlin, Epidemic threshold for the susceptible-infectious-susceptible model on random networks. *Phys. Rev. Lett.* **104**, 258701 (2010). doi:10.1103/PhysRevLett.104.258701 Medline

9. T. Harko, F. S. N. Lobo, M. K. Mak, Exact analytical solutions of the Susceptible-Infected-Recovered (SIR) epidemic model and of the SIR model with equal death and birth rates. *Appl. Math. Comput.* **236**, 184–194 (2014). doi:10.1016/j.amc.2014.03.030

10. T. Britton, P. D. O'Neill, Bayesian inference for stochastic epidemics in populations with random social structure. *Scand. J. Stat.* **29**, 375–390 (2002). doi:10.1111/1467-9469.00296

11. J. Lourenço, M. Maia de Lima, N. R. Faria, A. Walker, M. U. G. Kraemer, C. J. Villabona-Arenas, B. Lambert, E. Marques de Cerqueira, O. G. Pybus, L. C. J. Alcantara, M. Recker, Epidemiological and ecological determinants of Zika virus transmission in an urban setting. *eLife* **6**, e29820 (2017). doi:10.7554/eLife.29820 Medline

12. N. R. Faria, A. C. da Costa, J. Lourenço, P. Loureiro, M. E. Lopes, R. Ribeiro, C. S. Alencar, M. U. G. Kraemer, C. J. Villabona-Arenas, C.-H. Wu, J. Thézé, K. Khan, S. E. Brent, C. Romano, E. Delwart, B. Custer, M. P. Busch, O. G. Pybus, E. C. Sabino, NHLBI Recipient Epidemiology and Donor Evaluation Study-III (REDS-III), Genomic and epidemiological characterisation of a dengue virus outbreak among blood donors in Brazil. *Sci. Rep.* **7**, 15216 (2017). doi:10.1038/s41598-017-15152-8 Medline

13. B. Shulgin, L. Stone, Z. Agur, Pulse vaccination strategy in the SIR epidemic model. *Bull. Math. Biol.* **60**, 1123–1148 (1998). doi:10.1016/S0092-8240(98)90005-2 Medline

14. O. N. Bjørnstad, B. F. Finkenstadt, B. T. Grenfell, Dynamics of measles epidemics: Estimating scaling of transmission rates using a time series SIR model. *Ecol. Monogr.* **72**, 169–184 (2002). doi:10.1890/0012-9615(2002)072[0169:DOMEES]2.0.CO;2

15. L. Hufnagel, D. Brockmann, T. Geisel, Forecast and control of epidemics in a globalized world. *Proc. Natl. Acad. Sci. U.S.A.* **101**, 15124–15129 (2004). doi:10.1073/pnas.0308344101 Medline

16. A. Pandey, K. E. Atkins, J. Medlock, N. Wenzel, J. P. Townsend, J. E. Childs, T. G. Nyenswah, M. L. Ndeffo-Mbah, A. P. Galvani, Strategies for containing Ebola in West Africa. *Science* **346**, 991–995 (2014). doi:10.1126/science.1260612 Medline

17. R. Li, S. Pei, B. Chen, Y. Song, T. Zhang, W. Yang, J. Shaman, Substantial undocumented infection facilitates the rapid dissemination of novel coronavirus (SARS-CoV-2). *Science* **368**, 489–493 (2020). doi:10.1126/science.abb3221 Medline

18. A. J. Kucharski, T. W. Russell, C. Diamond, Y. Liu, J. Edmunds, S. Funk, R. M. Eggo; Centre for Mathematical Modelling of Infectious Diseases COVID-19 Working Group, Early dynamics of transmission and control of COVID-19: A mathematical modelling study. *Lancet Infect. Dis.* **20**, 553–558 (2020). doi:10.1016/S1473-3099(20)30144-4 Medline

19. J. Lourenco, R. Paton, M. Ghafari, M. Kraemer, C. Thompson, P. Simmonds, P. Klenerman, S. Gupta, Fundamental principles of epidemic spread highlight the immediate need for large-scale serological surveys to assess the stage of the SARS-CoV-2 epidemic. medRxiv 2020.03.24.20042291 [Preprint]. 26 March 2020; https://doi.org/10.1101/2020.03.24.20042291.

20. B. F. Maier, D. Brockmann, Effective containment explains subexponential growth in recent confirmed COVID-19 cases in China. *Science* eabb4557 (2020). doi:10.1126/science.abb4557 Medline

21. P. Bittihn, R. Golestanian, Containment strategy for an epidemic based on fluctuations in the SIR model. arXiv:2003.08784 [q-bio.PE] (19 March 2020).

22. R. M. Anderson, H. Heesterbeek, D. Klinkenberg, T. D. Hollingsworth, How will country-based mitigation measures influence the course of the COVID-19 epidemic? *Lancet* **395**, 931–934 (2020). doi:10.1016/S0140-6736(20)30567-5 Medline

23. J. R. Fauver, M. E. Petrone, E. B. Hodcroft, K. Shioda, H. Y. Ehrlich, A. G. Watts, C. B. F. Vogels, A. F. Brito, T. Alpert, A. Muyombwe, J. Razeq, R. Downing, N. R. Cheemarla, A. L. Wyllie, C. C. Kalinich, I. Ott, J. Quick, N. J. Loman, K. M. Neugebauer, A. L. Greninger, K. R. Jerome, P. Roychoundhury, H. Xie, L. Shrestha, M.-L. Huang, V. E. Pitzer, A. Iwasaki, S. B. Omer, K. Khan, I. Bogoch, R. A. Martinello, E. F. Foxman, M.-L. Landry, R. A. Neher, A. I. Ko, N. D. Grubaugh, Coast-to-coast spread of SARS-CoV-2 in the United States revealed by genomic epidemiology. medRxiv 2020.03.25.20043828 [Preprint]. 26 March 2020; https://doi.org/10.1101/2020.03.25.20043828.

24. A. Arenas, W. Cota, J. Gomez-Gardenes, S. Gómez, C. Granell, J. T. Matamalas, D. Soriano-Panos, B. Steinegger, A mathematical model for the spatiotemporal epidemic spreading of COVID19. medRxiv 2020.03.21.20040022 [Preprint]. 23 March 2020; https://doi.org/2020.03.21.20040022.

25. O. Mitjà, À. Arenas, X. Rodó, A. Tobias, J. Brew, J. M. Benlloch, 62 signatories, Experts' request to the Spanish Government: Move Spain towards complete lockdown. *Lancet* **395**, 1193–1194 (2020). doi:10.1016/S0140-6736(20)30753-4 Medline

26. S. L. Chang, N. Harding, C. Zachreson, O. M. Cliff, M. Prokopenko, Modelling transmission and control of the COVID-19 pandemic in Australia. arXiv:2003.10218 [q-bio.PE] (23 March 2020).

27. W. Bock, B. Adamik, M. Bawiec, V. Bezborodov, M. Bodych, J. P. Burgard, T. Goetz, T. Krueger, A. Migalska, B. Pabjan, T. Ozanski, E. Rafajlowicz, W. Rafajlowicz, E. Skubalska-Rafajlowicz, S. Ryfczynska, E. Szczurek, P. Szymanski, Mitigation and herd immunity strategy for COVID-19 is likely to fail. medRxiv 2020.03.25.20043109 [Preprint]. 5 May 2020; https://doi.org/10.1101/2020.03.25.20043109.

28. C. Gros, R. Valenti, L. Schneider, K. Valenti, D. Gros, Containment efficiency and control strategies for the Corona pandemic costs. arXiv:2004.00493 [physics.soc-ph] (1 April 2020).

29. V. Zlatić, I. Barjašić, A. Kadović, H. Štefančić, A. Gabrielli, Bi-stability of SUDR+K model of epidemics and test kits applied to COVID-19. arXiv:2003.08479 [q-bio.PE] (18 March 2020).

30. J. Dehning, J. Zierenberg, F. P. Spitzner, M. Wibral, J. Pinheiro Neto, M. Wilczek, V. Priesemann, Inferring COVID-19 spreading rates and potential change points for case number forecasts. arXiv:2004.01105 [q-bio.PE] (2 April 2020).

31. J. Dehning, F. P. Spitzner, J. Zierenberg, M. Wibral, J. Pinheiro Neto, M. Wilczek, V. Priesemann, Analysis code for: Inferring change points in the spread of COVID-19 reveals the effectiveness of interventions, Zenodo (2020); https://doi.org/10.5281/zenodo.3823382.

32. S. A. Lauer, K. H. Grantz, Q. Bi, F. K. Jones, Q. Zheng, H. R. Meredith, A. S. Azman, N. G. Reich, J. Lessler, The incubation period of coronavirus disease 2019 (COVID-19) from publicly reported confirmed cases: Estimation and application. *Ann. Intern. Med.* **172**, 577–582 (2020). doi:10.7326/M20-0504 Medline

33. J. Zhang, M. Litvinova, Y. Liang, Y. Wang, W. Wang, S. Zhao, Q. Wu, S. Merler, C. Viboud, A. Vespignani, M. Ajelli, H. Yu, Age profile of susceptibility, mixing, and social distancing shape the dynamics of the novel coronavirus disease 2019 outbreak in China. medRxiv 2020.03.19.20039107 [Preprint]. 20 March 2020; https://doi.org/10.1101/2020.03.19.20039107.

34. Y. Liu, A. A. Gayle, A. Wilder-Smith, J. Rocklöv, The reproductive number of COVID-19 is higher compared to SARS coronavirus. *J. Travel Med.* **27**, taaa021 (2020). doi:10.1093/jtm/taaa021 Medline

35. M. A. Muñoz, Colloquium: Criticality and dynamical scaling in living systems. *Rev. Mod. Phys.* **90**, 031001 (2018). doi:10.1103/RevModPhys.90.031001

36. A. Vehtari, A. Gelman, J. Gabry, Practical Bayesian model evaluation using leave-one-out cross-validation and WAIC. *Stat. Comput.* **27**, 1413–1432 (2017). doi:10.1007/s11222-016-9696-4

37. L. Peng, W. Yang, D. Zhang, C. Zhuge, L. Hong, Epidemic analysis of COVID-19 in China by dynamical modeling. arXiv:2002.06563 [q-bio.PE] (16 February 2020).

38. J. Wilting, V. Priesemann, Inferring collective dynamical states from widely unobserved systems. *Nat. Commun.* **9**, 2325 (2018). doi:10.1038/s41467-018-04725-4 Medline

39. Y.-C. Chen, P.-E. Lu, C.-S. Chang, T.-H. Liu, A Time-dependent SIR model for COVID-19 with undetectable infected persons. arXiv:2003.00122 [q-bio.PE] (28 February 2020).

40. E. Dong, H. Du, L. Gardner, An interactive web-based dashboard to track COVID-19 in real time. *Lancet Infect. Dis.* **20**, 533–534 (2020). doi:10.1016/S1473-3099(20)30120-1 Medline

41. M. Chinazzi, J. T. Davis, M. Ajelli, C. Gioannini, M. Litvinova, S. Merler, A. Pastore Y. Piontti, K. Mu, L. Rossi, K. Sun, C. Viboud, X. Xiong, H. Yu, M. E. Halloran, I. M. Longini Jr., A. Vespignani, The effect of travel restrictions on the spread of the 2019 novel coronavirus (COVID-19) outbreak. *Science* **368**, 395–400 (2020). doi:10.1126/science.aba9757 Medline

42. J. Salvatier, T. V. Wiecki, C. Fonnesbeck, Probabilistic programming in Python using PyMC3. *PeerJ Comput. Sci.* **2**, e55 (2016). doi:10.7717/peerj-cs.55

43. M. D. Hoffman, A. Gelman, The No-U-turn sampler: Adaptively setting path lengths in Hamiltonian Monte Carlo. *J. Mach. Learn. Res.* **15**, 1593–1623 (2014).

44. A. Kucukelbir, D. Tran, R. Ranganath, A. Gelman, D. M. Blei, Automatic differentiation variational inference. *J. Mach. Learn. Res.* **18**, 1–45 (2017).

45. K. L. Lange, R. J. A. Little, J. M. G. Taylor, Robust statistical modeling using the t Distribution. *J. Am. Stat. Assoc.* **84**, 881–896 (1989). doi:10.2307/2290063

46. S. di Santo, P. Villegas, R. Burioni, M. A. Muñoz, Simple unified view of branching process statistics: Random walks in balanced logarithmic potentials. *Phys. Rev. E* **95**, 032115 (2017). doi:10.1103/PhysRevE.95.032115 Medline

47. A. Gelman, Prior distributions for variance parameters in hierarchical models. *Bayesian Anal.* **1**, 515–534 (2006). doi:10.1214/06-BA117A

48. Johns Hopkins University, COVID-19 Data Repository by the Center for Systems Science and Engineering (CSSE) (2020); https://raw.githubusercontent.com/CSSEGISandData/COVID-19/bda67e3db0e8dca4540297633d431a8021c035c8/csse_covid_19_data/csse_covid_19_time_series/time_series_covid19_confirmed_global.csv.